Published in final edited form as:
NMR Biomed. 2014 August ; 27(8): 897–906. doi:10.1002/nbm.3133.

Dynamic Multi-Coil Technique (DYNAMITE) Shimming of the Rat Brain at 11.7 Tesla

Christoph Juchem[1], **Peter Herman**[1], **Basavaraju G. Sanganahalli**[1], **Peter B. Brown**[1], **Scott McIntyre**[1], **Terence W. Nixon**[1], **Dan Green**[2], **Fahmeed Hyder**[1], and **Robin A. de Graaf**[1]

[1]Yale University School of Medicine, Department of Diagnostic Radiology, MR Research Center (MRRC), 300 Cedar Street, New Haven, CT 06520, USA

[2]Agilent Technologies, Research Products Division, Yarnton, OX5 1QU, United Kingdom

Abstract

The *in vivo* rat model is a workhorse in neuroscience research, preclinical studies and drug development. A repertoire of MR tools has been developed for its investigation, however, high levels of B_0 magnetic field homogeneity are required for meaningful results. The homogenization of magnetic fields in the rat brain, i.e. shimming, is a difficult task due to a multitude of complex, susceptibility-induced field distortions. Conventional shimming with spherical harmonic (SH) functions is capable of compensating shallow field distortions in limited areas, e.g. in the cortex, but performs poorly in difficult-to-shim subcortical structures or for the entire brain. Based on the recently introduced multi-coil approach for magnetic field modeling, the *DYNA*mic *M*ulti-co*I*l *TE*chnique (DYNAMITE) is introduced for magnetic field shimming of the *in vivo* rat brain and its benefits for gradient-echo echo-planar imaging (EPI) are demonstrated.

An integrated multi-coil/radio-frequency (MC/RF) system comprising 48 individual localized DC coils for B_0 shimming and a surface transceive RF coil has been developed that allows MR investigations of the anesthetized rat brain *in vivo*. DYNAMITE shimming with this MC/RF setup is shown to reduce the B_0 standard deviation to a third of that achieved with current shim technology employing static first through third order SH shapes. The EPI signal over the rat brain increased by 31% and a 24% gain in usable EPI voxels could be realized.

DYNAMITE shimming is expected to critically benefit a wide range of preclinical and neuroscientific MR research. Improved magnetic field homogeneity, along with the achievable large brain coverage of this method will be crucial when signal pathways, cortical circuitry or the brain's default network are studied. Along with the efficiency gains of MC-based shimming compared to SH approaches demonstrated recently, DYNAMITE shimming has the potential to replace conventional SH shim systems in small bore animal scanners.

Keywords

shimming; dynamic shimming; magnetic field modeling; multi-coil; spherical harmonics

Address correspondence to: Christoph Juchem, MR Research Center (MRRC), 300 Cedar Street, TAC N142, New Haven, CT 06520, USA, Phone:+1 (203) 785-7021, Fax: +1 (203) 785-6643, christoph.juchem@yale.edu.

INTRODUCTION

The *in vivo* rat model is a workhorse in neuroscientific research, preclinical studies and drug development; and a repertoire of MR tools has been developed for its investigation. MR imaging (MRI) allows insights in the brain's anatomy, physiology and function with methods including echo-planar imaging (EPI) (1), diffusion tensor imaging (DTI) (2), MR spectroscopic imaging with one (3) or multiple spectral dimensions (4) and metabolic imaging e.g. with iron-oxide labeling (5). MR spectroscopy enables the quantification of the neurochemical profile (6-8) and sets the stage for the assessment of cellular metabolism, disease neuropathochemistry and drug functionality.

Functional MRI (fMRI) with Blood Oxygen Level-Dependent (BOLD) contrast is widely used to study sensory responses in the brain of anesthetized rats. Electrical forepaw or whisker and visual stimulation are the most frequently chosen activation models and produce well-defined BOLD signal increase in the primary somatosensory/visual cortices. Because different peripheral sensory pathways converge in subcortical regions, these brain structures are important sites for studying the interplay across different sensory modalities, sensory information processing and plasticity (9-17).

A multitude of shallow and complex magnetic field variations are apparent across the brain of the rat when placed in the magnetic field of an MR scanner (Fig. 1). These terms result from magnetic susceptibility differences within the rat anatomy and with respect to its surrounding. Particularly strong field terms are observed around air/tissue interfaces, e.g. close to the auditory tracts. MR methods based on spin echoes show some insensitivity towards magnetic field imperfection and the benefits e.g. of spin-echo BOLD imaging have been described recently (18). However, a large body of commonly applied MR methods demands high levels of magnetic field homogeneity for meaningful results. Among them, gradient-echo EPI (and fMRI) and the majority of spectroscopy techniques are the most prominent examples. For them, it is imperative to compensate the apparent field imperfections throughout the experiment. A complete cancellation of magnetic field variations requires the superposition of the identical field shape at reversed polarity. In reality, this process called magnetic field shimming is limited by the ability of the applied field synthesis to replicate the shape of the field distortion at hand. Deviations between the original field distortion and its best modeling representation remain as residual field imperfections after the shim process and can affect the MR investigation. To date, magnetic field shimming in the rat brain relies on spherical harmonic (SH) functions. With the use of first and second order SH terms, excellent magnetic field homogeneity is readily achieved in central areas of the rat brain (7) and in localized areas throughout the brain when strong and localized field artifacts are avoided (19; 20). This might be the reason why MR investigations are typically restricted to limited subsections of the brain such as elliptical ROIs in selected slices (20; 21). However, good magnetic field homogeneity is more difficult to achieve in brain regions that suffer from severe field artifacts and, moreover, over larger parts of the brain if such areas are included. While the study of subcortical regions is highly desirable, it is hard to achieve with conventional, SH-based shimming because of the complexity of the magnetic field artifacts apparent in these areas. Even magnetic field shimming with SH shapes up to the third order, i.e. the most powerful static

B_0 shimming currently available for rat preparations, is not capable of providing magnetic field homogeneity in the *in vivo* rat brain that is adequate for most MR investigations (Fig. 1).

Single-shot gradient-echo EPI, the prime tool for fMRI, is particularly susceptible to magnetic field imperfections. To date, the expectations of high-field MR applications have not been fully met in the rat brain, at least in part due to limited shimming. The ongoing trend towards ultra-high field (>15 Tesla) MR systems is expected to further amplify these problems (22). As such, there is a critical need for improved magnetic field homogenization in the rat brain.

We have shown recently that unrivaled magnetic field homogeneity can be achieved in the mouse and the human brain with static and dynamic multi-coil (MC) shimming (23; 24). Basis fields from local, individually driven coils are employed with the MC approach to synthesize the shim field for the problem at hand. The MC shim performance is based on the field modeling capability of the applied MC setup and can be further boosted by the dynamic application of MC shim fields in a time-varying, e.g. slice-specific, fashion. The aim of this study is to demonstrate the benefits of the *DYNA*mic *M*ulti-co*I*l *TE*chnique (DYNAMITE) for magnetic field shimming of the *in vivo* rat brain. Preliminary results of this work have been published in abstract form (25; 26).

METHODS

Integrated Multi-Coil and Radio-Frequency Setup

An integrated multi-coil and radio-frequency (MC/RF) system was developed for MR investigations of the *in vivo* rat brain at 11.7 Tesla (Fig. 2). The MC setup consisted of 48 individual copper coils of 30 turns that were wound from 0.4 mm diameter polyurethane/nylon coated copper magnet wire and mounted to the inside of an acrylic, cylindrical former with an inner diameter of 48 mm (Fig. 2). A single MC element was left out from the purely cylindrical MC design to allow space for the placement and integration of a surface ^{1}H RF coil (diameter 14 mm). Note that overlap and immediate proximity of the MC/RF coil systems was avoided to prevent RF-to-MC interactions and a reduction of the RF coils' transceive efficiency. The removed MC element was substituted by a coil that was placed outside the acrylic former. Its position and dimensions were chosen to provide a similar basis shape within the spatial volumes relevant for shimming. All 47 coils inside the MC former shared a 10 mm diameter while the single MC element on its outside had a diameter of 13 mm. Given the total coil thickness of about 3 mm, the distance between the inner coils and the isocenter of the magnet was 22 mm. Fully mounted, a 41 mm diameter cylindrical space remained open inside the MC/RF setup that allowed the placement of rats up to 350 g body weight along with further equipment. The latter included anesthesia tubing, physiological monitoring, along with optional devices for functional stimulation and extra- and/or intra-cranial electrophysiological recordings. Specific DYNAMITE shim fields were synthesized by driving the coils with a set of 48 optimized currents over a dynamic range of ±1 A as described in (23).

Animal Experiments

All procedures were performed in accordance with protocols approved by the Yale Institutional Animal Care and Use Committee and in agreement with the NIH guide for the care and use of laboratory animals. Experiments were conducted on twelve male Sprague-Dawley rats (weight 272 ± 27 g, mean ± SD, Charles River, Wilmington/MA, USA) which were anesthetized with isoflurane during surgery. Then the anesthesia was switched to urethane (1.3 g/kg i.p.) or α-chloralose (40 mg/kg/hr i.p.) and maintained during the sessions. Animals were tracheotomized and artificially ventilated (2% isoflurane during surgery + 70% N_2O/30% O_2). A femoral artery was cannulated for monitoring systemic parameters (blood pressure, pCO_2, pO_2, pH). The animals were placed on a heated pad to maintain their core temperature and an intravenous line was prepared for saline administration. All animals were used for a single experimental session only.

DYNAMITE Shimming for Echo-Planar Imaging (EPI)

Experiments were performed on a 11.7 Tesla magnet (Magnex Scientific, Oxford, UK) that was operated with VnmrJ 2.3A software (Agilent Technologies Inc., Santa Clara/CA, USA). The animals were fixated with a bite bar and a head holder on a cradle. The positioning of the cradle inside the MC/RF setup allowed the placement of the rat brain under the RF coil and the selection of an anterior-posterior portion of the brain. In this study, a central brain part around the bregma was considered. For magnetic field mapping, four single-echo GE images (FOV 26 × 26 × 12 mm^3, matrix 80 × 80 × 24, repetition time 1.3 s) were measured at relative echo time delays of 0/0.3/1/3 ms. Phase maps were calculated using voxel-by-voxel temporal phase unwrapping, before voxel-specific linear regression of signal phase and echo time was applied to derive 3-dimensional field maps (23). The decomposition of magnetic fields into the set of basis fields and the determination of the necessary coil currents for shimming was achieved by constrained least-squares fitting employing the Levenberg-Marquardt algorithm (27). A Matlab-based (MathWorks, Natick/MA, USA) software package B0DETOX (‘*beau-detox*’) was established in our laboratory to provide largely automated image reconstruction, region-of-interest (ROI) selection and magnetic field processing for both SH-based and DYNAMITE shimming. B0DETOX was operated on the MR scanner console for a streamlined determination of optimal shim settings at minimum user-interaction. The derived sets of 48 coil-specific currents for DYNAMITE shimming were uploaded to the MC shim interface via serial RS232 communication and played out during subsequent field mapping and EPI acquisitions based on sequence-initiated TTL triggering signals (23).

Any magnetic field variation within an MRI voxel leads to phase cancellation and signal dropout. The consideration of potential (through- or) intra-slice field components is of paramount importance for the successful application of dynamic slice shimming. If shim fields are determined from the 2-dimensional information of a single-slice field map (28; 29), potential intra-slice field gradients along the third, through-slice dimension are not considered and inevitably remain in experimental reality. In previous work, intra-slice components were measured along linear projections across the selected slice orientation, i.e. they were approximated by linear gradient terms (20; 30). Alternatively, additional slices before and after the slice-of-interest from the same multi-slice field mapping experiment

have been included to account for intra-slice artifacts up to the considered shim SH order (24; 31). Slices applied for EPI of the rat brain are typically broad compared to the dimensions of MRI slices applied for anatomical referencing and magnetic field mapping. In line with previous work from our laboratory (32; 33), a 2 mm slice thickness was chosen for EPI in this study as a compromise between anatomical specificity, attainable signal-to-noise ratio (SNR) and spatial coverage along the slice direction while avoiding inter-slice gaps. DYNAMITE shim fields for EPI were derived from field maps with 0.5 mm thick slices that were analyzed in groups of 4 to resemble the EPI slice geometry. Thereby intra-slice field behavior of the EPI slices was explicitly considered when field shapes for dynamic slice shimming were derived. This approach does not require any enlargement of the applied optimization volume as opposed to the inclusion of additional neighboring slices. The goal of this study was to benefit multi-slice EPI of the rat brain at 11.7 Tesla by improved magnetic field homogeneity. As such, magnetic field shimming of any given EPI slice was limited to the brain and only those field map voxels were considered that originated from brain locations.

DYNAMITE shimming was compared to static, third order SH shimming achieved with the scanners' built-in SH coil system with a dynamic range of X 3697 Hz/cm, Z 3719 Hz/cm, Y 3766 Hz/cm, X2-Y2 570 Hz/cm^2, ZX 1228 Hz/cm^2, Z2 2305 Hz/cm^2, ZY 1277 Hz/cm^2, XY 598 Hz/cm^2, X3 13.8 Hz/cm^3, Z(X2-Y2) 28.5 Hz/cm^3, Z2X 24.7 Hz/cm^3, Z3 81.9 Hz/cm^3, Z2Y 24.8 Hz/cm^3, ZXY 30.6 Hz/cm^3, Y3 14.2 Hz/cm^3 (all errors <1%). The shim outcome was assessed as standard deviation of the residual field distribution and through its impact on the quality of single-shot gradient-echo EPI of the *in vivo* rat brain. EPI parameters typical for fMRI of the rat brain at 11.7 Tesla were chosen (FOV 25.6x25.6x10/14 mm^3, matrix 64x64x5/7, TE 16 ms) and identical post-processing was applied to assure comparability.

RESULTS

DYNAMITE Shimming of the In Vivo Rat Brain

DYNAMITE shimming of the rat brain at the geometry of the original field map enabled largely improved magnetic field homogeneity (Fig. 3) compared to global SH shimming (Fig. 1). Not only were large-scale shallow field terms removed, but the strong and localized terms that remained with static SH shimming could also be successfully minimized (Table 1). Especially the severe field artifacts in the vicinity of the auditory tracts were largely reduced (red arrows). While major improvements in magnetic field homogeneity were achieved with DYNAMITE shimming, some extremely localized terms remained and perfect field homogeneity was not always achieved, e.g. at the immediate interface of brain tissue and air-filled auditory tracts.

Consistent with the high-resolution analysis of the shim outcome at the geometry of the field mapping experiment, third order SH shimming was found to remove the large-scale shallow field components from the bulk of the brain in the targeted EPI slices, but failed to correct for localized terms (Figs. 4). Even relatively shallow terms regularly remained in some areas after static SH shimming (SH Shim, slice 7) due to the multitude of distortions that magnetic field shimming faces throughout the rat brain.

Dynamic MC shimming largely eliminated the localized field terms (Fig. 4, DYNAMITE) and particularly alleviated the challenges associated to the large number of artifact areas (slice 7). For EPI, field inhomogeneity leads to phase cancellation and spatial misregistration. As such, the brain areas that contained residual field artifacts after SH shimming suffered from signal loss and image deformation (Fig. 5, SH Shim, slices 3/4).

The brain outline was largely preserved in DYNAMITE-shimmed EPI (Fig. 5, DYNAMITE, slices 3/4). While peripheral slices were regularly rendered useless with SH shimming (SH Shim, slice 7), DYNAMITE shimming allowed meaningful imaging throughout the sensitive area of the RF coil (DYNAMITE, slice 7). Signal increases were predominantly found in subcortical and peripheral brain areas (third row, DYNAMITE-minus SH-shimmed EPI). Note that alterations of the brain outline with SH shimming could lead to elevated apparent signals outside the brain (blue arrow).

Reasonable SNR is a basic prerequisite for any kind of MRI analysis. The impact of shimming on the EPI quality was therefore also assessed by the number of brain voxels with an SNR equal or larger than 10%, 20% and 30% of the maximal SNR observed in the brain. The inclusion of third order SH shapes in the shimming process reduced the average standard deviation of the observed field values by 12% compared to second order SH shimming (Table 2), but the number of suitable brain voxels was only marginally increased by 0-2%. In other words, areas of strong and localized field gradients remained largely unaffected by these improvements, critical intra-voxel signal cancellation was not significantly affected and only a few voxels could be recovered. DYNAMITE shimming allowed improved field homogeneity throughout the brain and, more importantly, the compensation of the severe field gradients close to the brain surface. Consequently, the outline of the brain could be largely preserved. The amount of usable EPI voxels with a signal intensity of at least 10%, 20% and 30% of the maximum value was increased by 19%, 26% and 28%, respectively, with an overall increase of (24 ± 7)%. The mean signal increase with DYNAMITE compared to static third order SH shimming was found to be (31 ± 17)%. The exact homogeneity gain was dependent on the details of the considered brain anatomy and the field imperfections therein.

Extreme Shim Challenge: Steel Electrodes for Whisker Stimulation

The motivation for the development of the MC/RF setup was to establish an experimental platform for multimodal neuroscience experiments in the anesthetized rat. The current installation allows the inclusion of extra-cranial (EEG) or intracranial electrodes for electrophysiological recording and additional hardware for forepaw or whisker stimulation.

To date, the use of magnetic materials in the scanner environment is largely prohibitive. The employed parts and materials were therefore carefully selected to ensure negligible impact on the static B_0 field distribution within the rat brain. If typically applied components (hardware, gels, cement) were allowed to be magnetic, a greater experimental flexibility could be achieved. To this end, an extreme example of such scenario was mimicked by replacing a pair of non-magnetic tungsten electrodes for whisker stimulation by models made of steel. Note that there is no immediate benefit to the selected problem. The sole motivation of this example is to demonstrate the general ability of DYNAMITE shimming

to cope with demanding field distortions and the role it can play in relaxing the overall ban of magnetic materials from the MR environment. The electrodes (length 11.3 mm, diameter 0.35 mm) were inserted sub-dermally above and below the right whisker pad, parallel to row A and E with the tips reaching the height of the nose. The ability of the DYNAMITE setup and approach to cope with such severe shim challenge was then tested and compared to SH-based shimming. The field distortion that the steel electrode induced in the rat brain spanned a frequency range of a couple thousand Hertz (Fig. 6A). Similar to the regular brain shimming scenario, four field map slices resembled the geometry of every EPI slice. Significant field imperfections remained within EPI slices throughout the brain with second order SH shimming (Fig. 6B). The combination of in-slice imperfections and through-slice components, i.e. field variations across the four field maps contributing to the same EPI slice, led to severe image distortion and signal dropout with EPI. While not perfect, DYNAMITE shimming was capable of removing large part of both the electrode- and the anatomy-induced field terms and allowed meaningful EPI quality throughout the brain even under these extreme conditions (Fig. 6C).

DISCUSSION

Magnetic field conditions in the *in vivo* rat brain are characterized by a large number of localized field terms of varying polarity that span the brain's surface. Field modeling with up to third order SH shapes is incapable of fully resembling these field artifacts. The inclusion of higher order SH shapes improves the shim performance, but the attainable gains are limited by the complexity and, more importantly, the spatial spread of field artifacts for the problem at hand (Fig. 1, Table 1). SH field modeling is primarily limited in shaping the required shim field rather than in providing its amplitude. The down-scaling of a SH coil system from the size of the scanner bore to the size of the applied MC setup leads to efficiency gains, i.e. higher SH amplitudes per unit current. However, the shapes of the generated fields as well as the shim outcome are expected to remain unchanged as SH fields are self-similar (34). The analysis of SH shimming in this work assumes an infinite amplitude range for all terms. The results therefore describe the best-case scenario and might be further compromised if the necessary amplitude range is not available in reality. The details of the static SH shim performance depend on the size and considered portion of the brain ROI and better field homogeneity is expected for smaller ROIs similar to the ROI fragmentation with dynamic approaches. Notably, the performance of dynamic shimming is independent of the dorso-ventral extension of the considered brain ROI, while the attainable field homogeneity with static shimming is further reduced with larger slice stacks.

DYNAMITE shimming was compared to third order SH shimming as this is the best currently available method for global magnetic field homogenization of the *in vivo* rat brain (21; 35). Dynamic shimming is inherently more powerful than the static use of the identical set of basis shapes irrespective of the method applied. Dynamic SH shimming (or "Dynamic Shim Updating", DSU) has been used in the human brain to achieve improved magnetic field homogeneity with the application of first (36; 37), second (30) and third order (31) SH functions. Magnetic field terms encountered in the human brain are largely shallow with few exceptions in prefrontal cortex and the temporal lobes. Instead, the rat brain suffers from a multitude of field terms that are distributed throughout the brain. Therefore, dynamic

shimming proves particularly beneficial in the rat brain as it allows to separate the overall field distribution into more manageable subunits. As such, dynamic SH shimming could be an alternative option and its benefits have been demonstrated in the rat brain before (20). However, current dynamic SH implementations are based on bore-sized SH coils that face technical challenges, e.g. the generation of eddy currents, which are negligible for the presented DYNAMITE approach. More importantly, although SH-based dynamic shimming has been presented up to the third order for the human brains, no such implementation exists yet for small bore MR systems.

The field shaping capacity of the MC approach does not critically rely on the number, size and positioning of the applied coil setup or the geometry of the individual coils as long as a reasonably diverse repertoire of shapes is generated (34). The theoretical design of the MC setup in this study was therefore dominated by engineering decisions for the placement of the coils to the available space around the rat head along with numerical simulations of the shimming process to optimize the DYNAMITE shim outcome. Individual MC basis fields from localized coils provide distinct spatial patterns close to the coils and more shallow components farther away. The most complex magnetic field shapes can therefore be generated at reasonable proximity to the coils. The small portion of the rat head covered by the rats' brain, e.g. compared to the mouse or the human, poses a limitation to the performance of MC-based magnetic field modeling and shimming. More importantly, the most challenging field artifacts in the rat brain are located deep inside the head close to the auditory tracts. Their distance to the head surface and the MC system therefore limits the available field modeling capability and the attainable shim outcome in these brain areas. Despite these challenges, DYNAMITE shimming with the presented MC/RF setup is expected to outperform even fourth order dynamic SH shimming (Table 2).

The MC/RF setup was designed to benefit MR investigations targeting the *in vivo* rat brain at 11.7 Tesla and improved EPI quality has been demonstrated in a first application. Anesthetized rat preparations for neuroscience research are generally demanding due to the multitude of procedures and hardware involved. The application of the presented MC/RF setup added 10-15 min to a typical preparation time for a comparable RF-only setup. In this study, shim fields were specifically tailored to the rat brain. While the magnetic field conditions outside the brain were not explicitly controlled, no artifacts such as image folding were observed due to magnetic field behavior in non-brain areas. In line with previous work on the mouse brain (23), DYNAMITE shim fields targeting the rat brain commonly implicated severe gradient terms outside the brain that acted as phase spoilers. The explicit spoiling of non-brain magnetization can be included in the shim procedure for zoomed MRI applications and to reduce acquisition times. If necessary, amplitude and/or gradient boundaries can be imposed onto non-ROI areas in the computational procedures. Their inclusion, however, implies an ROI enlargement which inevitably affects the shim performance inside the brain.

A 14 mm diameter ^{1}H surface RF coil has been integrated with the MC setup in this study. This choice represents a trade-off between RF sensitivity, depth profile of the RF coil and the attainable dorso-ventral coverage of the rat brain while avoiding uncovered gaps between slices (32; 33). The flexibility of the coil placement with the MC approach allowed

the integration of both systems without compromising the RF coil positioning or performance. The extension of the suitable dorso-ventral FOV with the presented MC/RF implementation is limited to approximately 14 mm (or seven 2-mm EPI slices) due to the limited sensitivity of the applied surface coil. The ROI example presented here focused on the central brain, but other brain areas can be studied by appropriate head positioning. DYNAMITE-shimming with the presented MC/RF setup is by no means limited to the applied slice orientation and other orientations have been realized already, e.g. coronal slicing for fMRI of cortical layers (data not shown).

Also, other RF coil geometries are expected to be realizable with an adaptation of the MC/RF design and architecture. Theoretical magnetic field shimming with a simple 48-element MC design (13 mm coil diameter, 30 turns, ±1 A range, regular grid) placed on a cylindrical surface with a 6-cm diameter reduced the magnetic field imperfections in the rat brain to 46 ± 7 Hz and 24 ± 4 Hz with static MC and DYNAMITE shimming, respectively (compare Table 2). The field homogeneity that can be expected from MC shimming with such large-diameter setup still compares to fourth SH order static and dynamic shimming, respectively. Note that MC shimming benefits from a reasonable proximity of the MC setup to the ROI by an increased diversity of field shapes, however, it does not solely rely on it. The above example illustrates the interplay of the basic aspects of DYNAMITE shimming when compared to the MC design applied in this study, namely the repertoire of distinct and complex shapes (as a result of a close coil positioning), the MC approach for magnetic field modeling and the break-down of the ROI at hand in virtual subunits with dynamic shimming. More importantly, the realization of the benefits of MC shimming in larger setups opens the door towards their design and placement around volume RF coils (23), RF coil arrays or combinations thereof. Such MC/RF setups are expected to provide optimal RF sensitivity along with improved B_0 field homogeneity.

In a proof-of-principle application, the ability of DYNAMITE shimming to cope with the severe field distortion induced by magnetic stimulation electrodes was demonstrated. This extreme example also illustrated the excess buffer of the implementation with respect to the shim field amplitudes that can be generated with a limited 1 Ampere current range. Notably, some SH amplifiers started to oscillate with the application of the required first-through-third order fields. Therefore, the SH-shimmed field maps and EPI images (Fig. 6B) consider first-through-second order SH terms only (based on the appropriate second order analysis). The theoretical analysis showed that largely identical performances were expected from second and third order SH shimming with a further narrowing of the standard deviation of the residual field distribution by less than 2%. This negligible net gain with the inclusion of third order terms is due to the multitude of localized field artifacts which are far beyond the shaping capability of both second and third order SH shimming.

Artifacts in EPI and other MR methods susceptible to magnetic field imperfections can be reduced by the appropriate choice of the MR acquisition parameters (38). For instance, improved spatial resolution, i.e. decreased voxel volumes, minimizes intra-voxel magnetic field variations and the concomitant signal dephasing. An increased acquisition bandwidth reduces spatial misregistration and image deformation. The parameter choice in this study was based on an EPI protocol commonly used in our laboratory for fMRI of the rat brain and

a further optimization, e.g. of the applied FOV, might be possible. However, these efforts typically come at the price of reduced SNR, extended acquisition time or increased demands on the scanners' gradient performance. More importantly, any MR investigation relies on optimal parameter choices to derive the most meaningful results for the application at hand. The need to tailor the experimental details to the minimization of artifacts potentially compromises the achievable study outcome.

Post-processing image corrections can compensate – within limits – spatial mis-registration of MR signals. Since signal loss is not recovered by any post-processing method, only the experimental minimization of the responsible magnetic field distortion by magnetic field shimming can provide a true remedy. Both SNR and image quality of EPI were shown in this study to benefit significantly from DYNAMITE shimming. More importantly, DYNAMITE shimming enabled reasonable SNR even in areas of severe and complex field distortions. SNR also depends on factors other than shimming such as the sensitivity profile of the applied RF coil. The disentanglement of such effects, however, has not been intended here. Notably, the residual field deviations after DYNAMITE shimming were highly predictable and, therefore, further improvements in image quality are expected with their consideration in the spatial reconstruction.

Multimodal stimulation paradigms lead to functional activation in the primary brain regions, but also activate additional integration areas. As such, localized shimming of individual target brain areas becomes progressively problematic as the limitation to a limited number of easy-to-shim areas bears the risk of missing out on relevant information. DYNAMITE shimming with the developed MC/RF setup enables MR investigations with significant brain coverage. The study of the default network, brain connectivity and multimodal integration with EPI-based fMRI are expected to particularly benefit from DYNAMITE shimming.

This research focused on magnetic field shimming in the rat brain due to its key role in neuroscientific research. However, DYNAMITE shimming is by no means limited to the brain. The developed technology and methods are expected to be readily applicable to other parts of the rat body, e.g. for metabolic studies of rat skeletal muscle (39), or and for MR applications addressing the mouse body (40). The available short switching times of the current implementation (10 μs, full range) furthermore provide the basis for real-time shimming, e.g. for the compensation of respiration-induced B_0 variations, similar to human applications (41).

Rat anatomy and external hardware are not the only possible origins for magnetic field perturbations in the rat brain. While microscopic field perturbations from iron-oxide-based contrast agents are desired, the large-scale macroscopic field alterations associated to severe iron-load are not (Figs. 7A/B). Such field distortions can largely exceed the immediate location of the contrast agent and therefore cause signal dephasing and image distortions even in distant areas. The macroscopic field terms induced by iron-oxide contrast agents tend to be extremely complex (e.g. with intra-ventricular injections) and their complete compensation is unlikely with any shimming method. However, simulations suggest that the DYNAMITE approach has the potential to alleviate the problems in neighboring areas to a level that concomitant MRI artifacts are minimized (Fig. 7C).

In summary, DYNAMITE shimming of the *in vivo* rat brain has been introduced and the benefits compared to conventional SH-based techniques have been demonstrated. Along with the efficiency gains of MC-based shimming compared to SH approaches shown recently (34), the multi-coil technology has the potential to replace conventional SH shim systems in small bore animals scanners. DYNAMITE shimming is expected to benefit a wide range of biomedical MR research and to be crucial when signal pathways, cortical circuitry, the brain's default network or multi-modal integration are studied.

Acknowledgments

The authors would like to thank Bei Wang for expert animal handling, Dr. Dorit Granot for obtaining magnetic field information from iron-oxide-labeled rat brain and Dr. Paul Kinchesh (Agilent Technologies) for helpful discussions on EPI. This research was supported by NIH grants R21/R33-CA118503, P30-NS052519, R01-EB000473 and R01-EB014861, and Agilent Technologies Inc..

Abbreviations

fMRI	functional MRI
BOLD	blood oxygen level dependence
EPI	echo-planar imaging
SH	spherical harmonics
MC	multi-coil
DYNAMITE	dynamic multi-coil technique

References

1. Sanganahalli BG, Bailey CJ, Herman P, Hyder F. Tactile and non-tactile sensory paradigms for fMRI and neurophysiologic studies in rodents. Methods Mol Biol. 2009; 489:213–242. [PubMed: 18839094]
2. Chahboune H, Mishra AM, DeSalvo MN, Staib LH, Purcaro M, Scheinost D, Papademetris X, Fyson SJ, Lorincz ML, Crunelli V, Hyder F, Blumenfeld H. DTI abnormalities in anterior corpus callosum of rats with spike-wave epilepsy. Neuroimage. 2009; 47(2):459–466. [PubMed: 19398019]
3. Dreher W, Leibfritz D. Fast proton spectroscopic imaging with high signal-to-noise ratio: spectroscopic RARE. Magn Reson Med. 2002; 47(3):523–528. [PubMed: 11870839]
4. von Kienlin M, Ziegler A, Le Fur Y, Rubin C, Decorps M, Remy C. 2D-spatial/2D-spectral spectroscopic imaging of intracerebral gliomas in rat brain. Magn Reson Med. 2000; 43(2):211–219. [PubMed: 10680684]
5. Shapiro EM, Skrtic S, Koretsky AP. Sizing it up: cellular MRI using micron-sized iron oxide particles. Magn Reson Med. 2005; 53(2):329–338. [PubMed: 15678543]
6. Pfeuffer J, Tkac I, Provencher SW, Gruetter R. Toward an in vivo neurochemical profile: quantification of 18 metabolites in short-echo-time (1)H NMR spectra of the rat brain. J Magn Reson. 1999; 141(1):104–120. [PubMed: 10527748]
7. Tkac I, Starcuk Z, Choi IY, Gruetter R. In vivo 1H NMR spectroscopy of rat brain at 1 ms echo time. Magn Reson Med. 1999; 41(4):649–656. [PubMed: 10332839]
8. de Graaf RA, Mason GF, Patel AB, Rothman DL, Behar KL. Regional glucose metabolism and glutamatergic neurotransmission in rat brain in vivo. Proc Natl Acad Sci U S A. 2004; 101(34): 12700–12705. [PubMed: 15310848]

9. Devor A, Ulbert I, Dunn AK, Narayanan SN, Jones SR, Andermann ML, Boas DA, Dale AM. Coupling of the cortical hemodynamic response to cortical and thalamic neuronal activity. Proc Natl Acad Sci U S A. 2005; 102(10):3822–3827. [PubMed: 15734797]
10. Laurienti PJ, Perrault TJ, Stanford TR, Wallace MT, Stein BE. On the use of superadditivity as a metric for characterizing multisensory integration in functional neuroimaging studies. Exp Brain Res. 2005; 166(3-4):289–297. [PubMed: 15988597]
11. Meredith MA, Stein BE. Visual, auditory, and somatosensory convergence on cells in superior colliculus results in multisensory integration. J Neurophysiol. 1986; 56(3):640–662. [PubMed: 3537225]
12. Alvarado JC, Rowland BA, Stanford TR, Stein BE. A neural network model of multisensory integration also accounts for unisensory integration in superior colliculus. Brain Res. 2008; 1242:13–23. [PubMed: 18486113]
13. Olavarria J, Van Sluyters RC, Killackey HP. Evidence for the complementary organization of callosal and thalamic connections within rat somatosensory cortex. Brain Res. 1984; 291(2):364–368. [PubMed: 6697197]
14. Brett-Green B, Fifkova E, Larue DT, Winer JA, Barth DS. A multisensory zone in rat parietotemporal cortex: intra- and extracellular physiology and thalamocortical connections. J Comp Neurol. 2003; 460(2):223–237. [PubMed: 12687687]
15. Grunwerg BS, Krauthamer GM. Vibrissa-responsive neurons of the superior colliculus that project to the intralaminar thalamus of the rat. Neurosci Lett. 1990; 111(1-2):23–27. [PubMed: 2336187]
16. Alloway KD, Olson ML, Smith JB. Contralateral corticothalamic projections from MI whisker cortex: potential route for modulating hemispheric interactions. J Comp Neurol. 2008; 510(1): 100–116. [PubMed: 18615539]
17. Bailey CJ, Sanganahalli BG, Herman P, Blumenfeld H, Gjedde A, Hyder F. Analysis of time and space invariance of BOLD responses in the rat visual system. Cereb Cortex. 2013; 23(1):210–222. [PubMed: 22298731]
18. Zhao F, Wang P, Hendrich K, Ugurbil K, Kim SG. Cortical layer-dependent BOLD and CBV responses measured by spin-echo and gradient-echo fMRI: insights into hemodynamic regulation. Neuroimage. 2006; 30(4):1149–1160. [PubMed: 16414284]
19. Tkac I, Rao R, Georgieff MK, Gruetter R. Developmental and regional changes in the neurochemical profile of the rat brain determined by in vivo 1H NMR spectroscopy. Magn Reson Med. 2003; 50(1):24–32. [PubMed: 12815675]
20. de Graaf RA, Brown PB, McIntyre S, Rothman DL, Nixon TW. Dynamic shim updating (DSU) for multislice signal acquisition. Magn Reson Med. 2003; 49(3):409–416. [PubMed: 12594742]
21. Miyasaka N, Takahashi K, Hetherington HP. Fully automated shim mapping method for spectroscopic imaging of the mouse brain at 9.4 T. Magn Reson Med. 2006; 55(1):198–202. [PubMed: 16270332]
22. Shajan G, Hoffmann J, Balla DZ, Deelchand DK, Scheffler K, Pohmann R. Rat brain MRI at 16.4T using a capacitively tunable patch antenna in combination with a receive array. NMR Biomed. 2012; 25(10):1170–1176. [PubMed: 22344898]
23. Juchem C, Brown PB, Nixon TW, McIntyre S, Rothman DL, de Graaf RA. Multi-coil shimming of the mouse brain. Magn Reson Med. 2011; 66(3):893–900. [PubMed: 21442653]
24. Juchem C, Nixon TW, McIntyre S, Boer VO, Rothman DL, de Graaf RA. Dynamic multi-coil shimming of the human brain at 7 Tesla. J Magn Reson. 2011; 212:280–288. [PubMed: 21824794]
25. Juchem C, Sanganahalli BG, Herman P, Brown PB, McIntyre S, Nixon TW, de Graaf RA. Dynamic Multi-Coil Shimming of the Rat Brain at 11.7 Tesla. Proc ISMRM, Salt Lake City, USA. 2013:0667.
26. Juchem, C.; Herman, P.; Sanganahalli, BG.; Nixon, TW.; Brown, PB.; McIntyre, S.; Hyder, F.; de Graaf, RA. Proc ISMRM. Milan, Italy: 2014. Dynamic Multi-Coil Technique (DYNAMITE) Shimmed EPI of the Rat Brain at 11.7 Tesla; p. 2983
27. Juchem C, Nixon TW, McIntyre S, Rothman DL, de Graaf RA. Magnetic field modeling with a set of individual localized coils. J Magn Reson. 2010; 204(2):281–289. [PubMed: 20347360]
28. Harris CT, Handler WB, Chronik BA. A new approach to shimming: The dynamically controlled adaptive current network. Magn Reson Med. 2013

29. Han H, Song AW, Truong TK. Integrated parallel reception, excitation, and shimming (iPRES). Magn Reson Med. 2013; 70:241–247. [PubMed: 23629974]
30. Koch KM, McIntyre S, Nixon TW, Rothman DL, de Graaf RA. Dynamic shim updating on the human brain. J Magn Reson. 2006; 180(2):286–296. [PubMed: 16574443]
31. Juchem C, Nixon TW, Diduch P, Rothman DL, Starewicz P, de Graaf RA. Dynamic shimming of the human brain at 7 Tesla. Concepts Magn Reson. 2010; 37B(3):116–128.
32. Sanganahalli BG, Herman P, Hyder F, S KS. Mitochondrial calcium uptake capacity modulates neocortical excitability. JCBFM. 2013; 33(7):1115–1126.
33. Sanganahalli BG, Herman P, Behar KL, Blumenfeld H, Rothman DL, Hyder F. Functional MRI and neural responses in a rat model of Alzheimer's disease. NeuroImage. 2013; 79:401–411.
34. Juchem C, Green D, de Graaf RA. Multi-coil magnetic field modeling. J Magn Reson. 2013; 236:95–104. [PubMed: 24095841]
35. Chen Z, Li SS, Yang J, Letizia D, Shen J. Measurement and automatic correction of high-order B0 inhomogeneity in the rat brain at 11.7 Tesla. Magn Reson Imaging. 2004; 22(6):835–842. [PubMed: 15234452]
36. Blamire AM, Rothman DL, Nixon T. Dynamic shim updating: a new approach towards optimized whole brain shimming. Magn Reson Med. 1996; 36(1):159–165. [PubMed: 8795035]
37. Morrell G, Spielman D. Dynamic shimming for multi-slice magnetic resonance imaging. Magn Reson Med. 1997; 38(3):477–483. [PubMed: 9339449]
38. Speck O, Stadler J, Zaitsev M. High resolution single-shot EPI at 7T. Magma. 2008; 21(1-2):73–86. [PubMed: 17973132]
39. De Feyter HM, Lenaers E, Houten SM, Schrauwen P, Hesselink MK, Wanders RJ, Nicolay K, Prompers JJ. Increased intramyocellular lipid content but normal skeletal muscle mitochondrial oxidative capacity throughout the pathogenesis of type 2 diabetes. Faseb J. 2008; 22(11):3947–3955. [PubMed: 18653763]
40. Bakermans AJ, van Weeghel M, Denis S, Nicolay K, Prompers JJ, Houten SM. Carnitine supplementation attenuates myocardial lipid accumulation in long-chain acyl-CoA dehydrogenase knockout mice. J Inherit Metab Dis. 2013; 36(6):973–981. [PubMed: 23563854]
41. van Gelderen P, de Zwart JA, Starewicz P, Hinks RS, Duyn JH. Real-time shimming to compensate for respiration-induced B0 fluctuations. Magn Reson Med. 2007; 57(2):362–368. [PubMed: 17260378]

- An integrated DC multi-coil/radio-frequency system for MR investigations of the *in vivo* rat brain at 11.7 Tesla is presented and the benefits of DYNAMITE (*DYNA*mic *M*ulti-co*I*l *TE*chnique) B_0 shimming are demonstrated.
- Improved whole-brain EPI quality is expected to critically benefit a wide range of preclinical MR research and will be crucial when signal pathways, cortical circuitry or the brain's default network are studied.
- DYNAMITE shimming has the potential to replace conventional shim systems in small bore animal scanners.

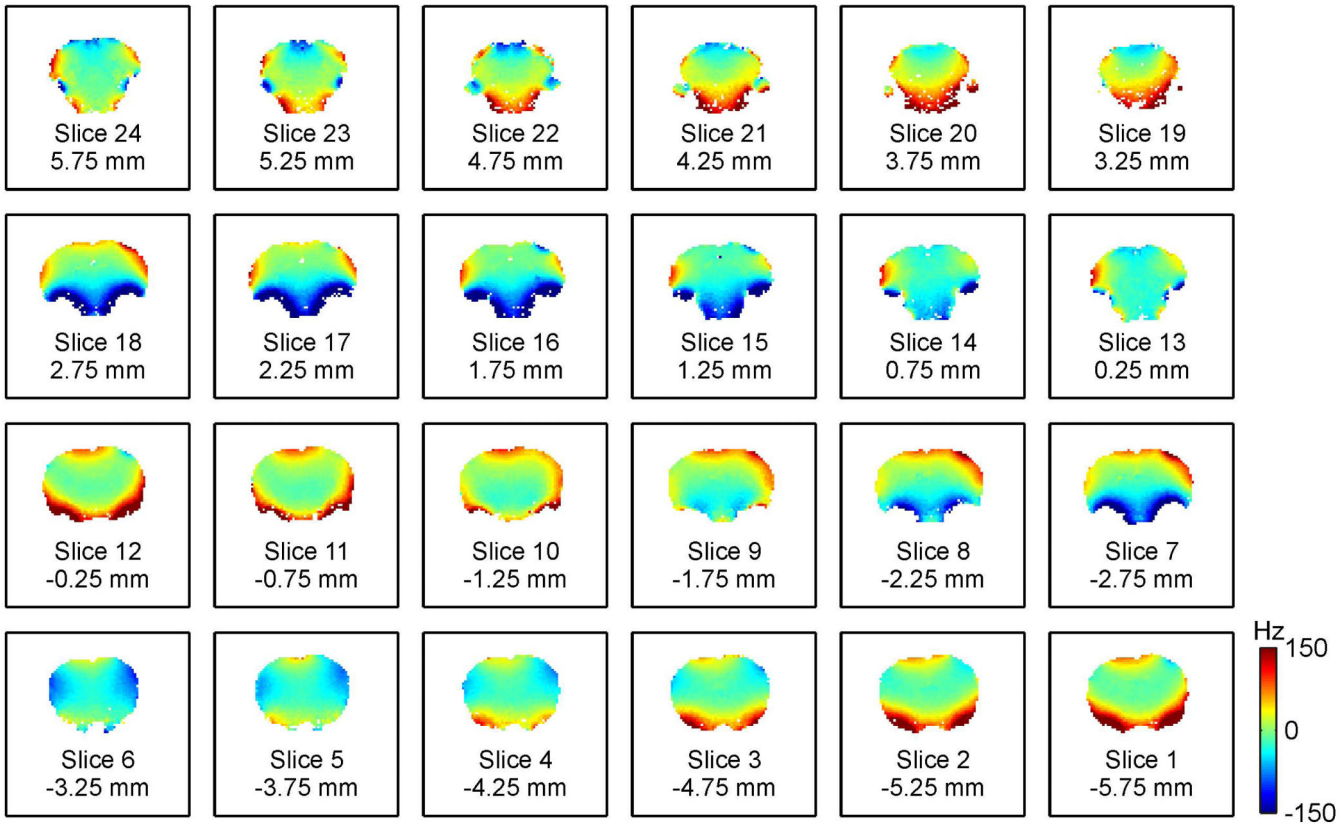

Fig. 1. GLOBAL SH SHIMMING OF THE RAT BRAIN

Magnetic field shimming of the rat brain at 11.7 Tesla with first-through-third order SH shapes. Global SH shimming removes the bulk of the field inhomogeneity, but fails to address the localized terms of varying polarity that are found throughout the brain.

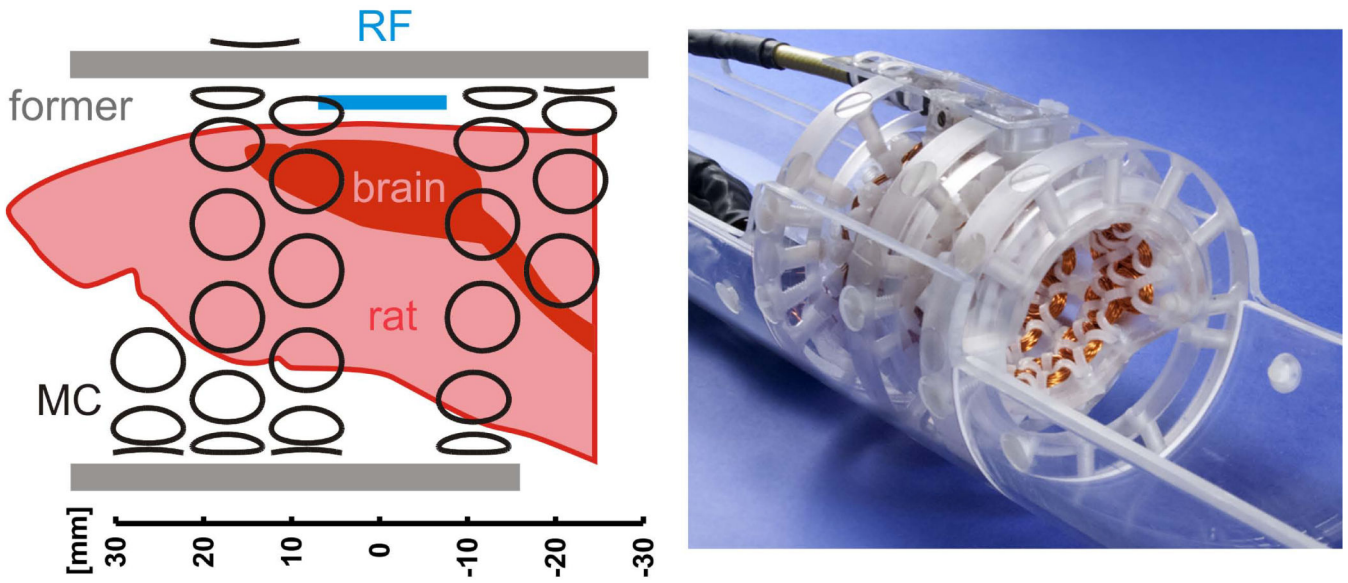

Fig. 2. EXPERIMENTAL COIL SETUP

Integrated multi-coil/radio-frequency (MC/RF) setup for MR investigations of the rat brain at 11.7 Tesla. Left: A 14 mm diameter surface RF coil (blue) is integrated with a dedicated 48-coil setup (black) for DYNAMITE shimming. Right: In its experimental realization, the MC setup is mounted on the inside of an acrylic former. The available cylindrical space (diameter 41 mm) allows the placement of a rat along with further equipment for animal handling (e.g. cradle, bite bar, heating pad), maintenance of anesthesia, physiological supervision and hardware for functional stimulation.

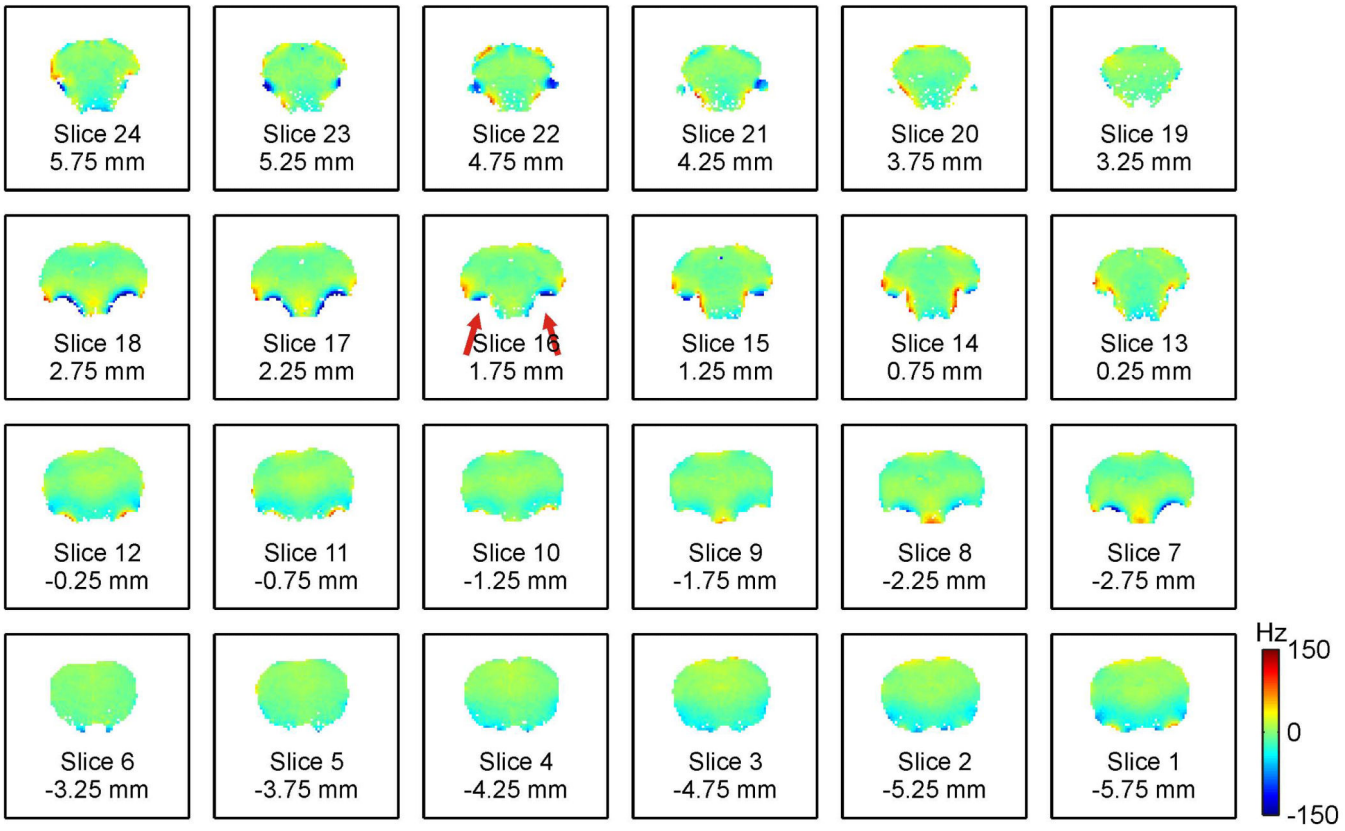

Fig. 3. DYNAMITE SHIMMING OF THE RAT BRAIN

Dynamic multi-coil technique (DYNAMITE) for magnetic field shimming of the rat brain at 11.7 Tesla. Slice-by-slice shimming at the geometry of the original field map removed the bulk of the field inhomogeneity and minimized the localized terms throughout the brain (compare to Fig. 1).

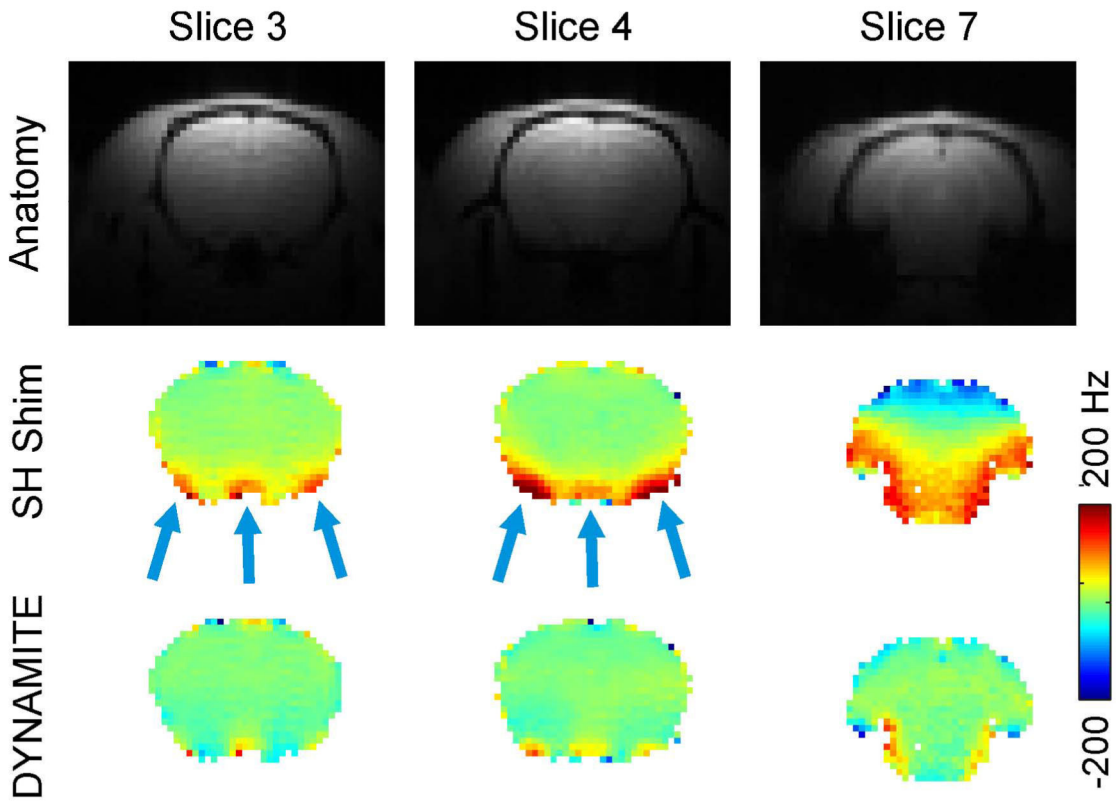

Fig. 4. DYNAMITE VS. SH SHIMMING FOR EPI

Comparison of SH and DYNAMITE magnetic field shimming. First row: Standard gradient-echo structural images of the rat brain. Center row: Localized field imperfections of varying polarity remain in the rat brain at 11.7 Tesla after static (global) first through third order spherical harmonic (SH) shimming, since the complexity of the distortions exceeds the modeling capability of SH field shaping. Third row: The combination of MC field modeling and a dynamic approach for shimming enables largely improved magnetic field homogeneity throughout the brain.

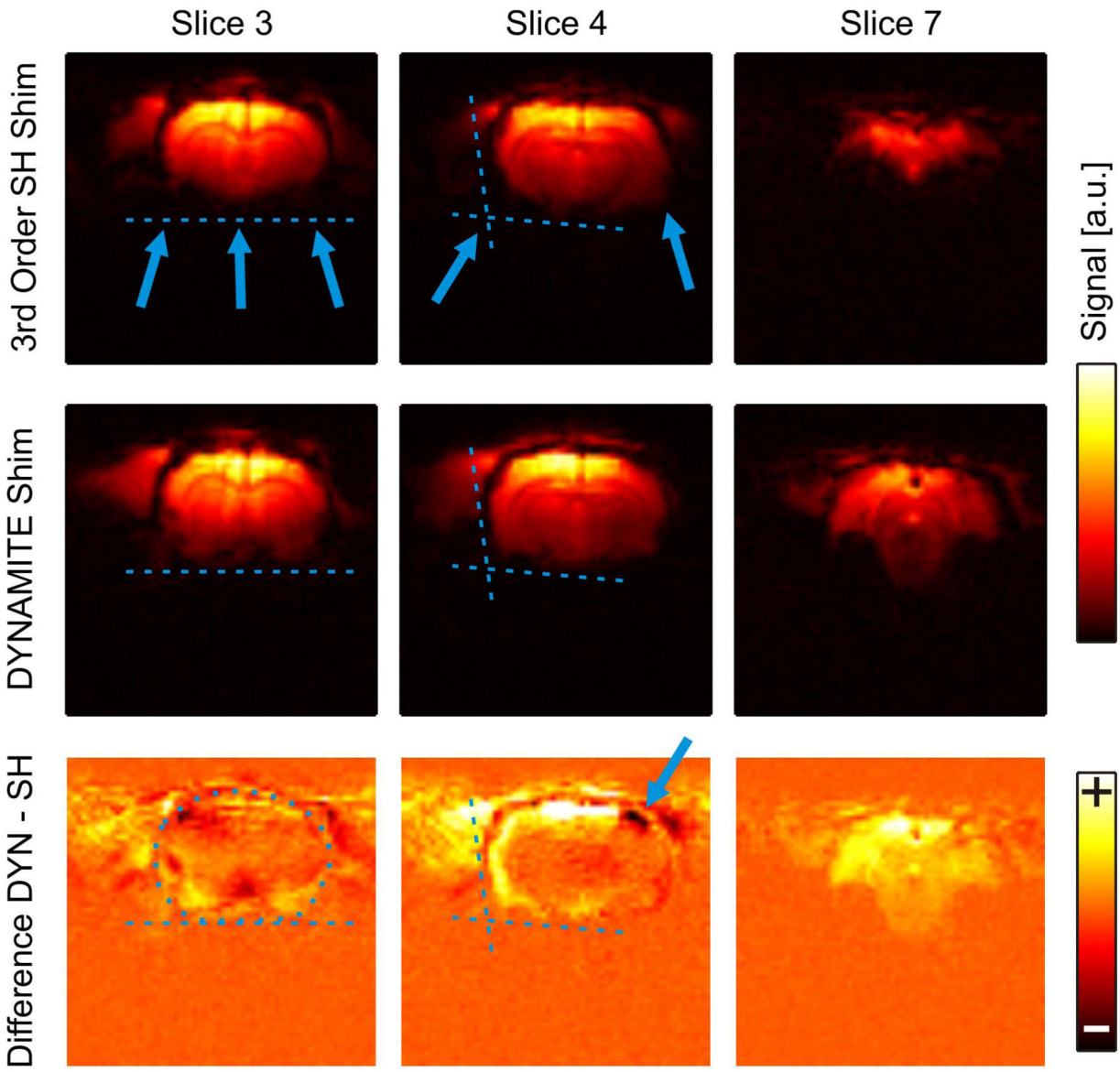

Fig. 5. DYNAMITE- VS. SH-SHIMMED EPI

Impact of magnetic field homogeneity on the image quality of gradient-echo EPI. Signal cancellation is observed with conventional SH shimming and significant parts of subcortical and peripheral brain areas have vanished (first row). Dynamic multi-coil (DYNAMITE) shimming minimized EPI signal loss and largely preserved the outline of the brain even close to severe susceptibility interfaces and in peripheral slices (second row). Signal increases were predominantly found in subcortical and peripheral brain areas (third row, DYNAMITE-minus SH-shimmed EPI). Note that alterations of the brain outline with SH shimming could lead to elevated apparent signals at the brain border (blue arrow).

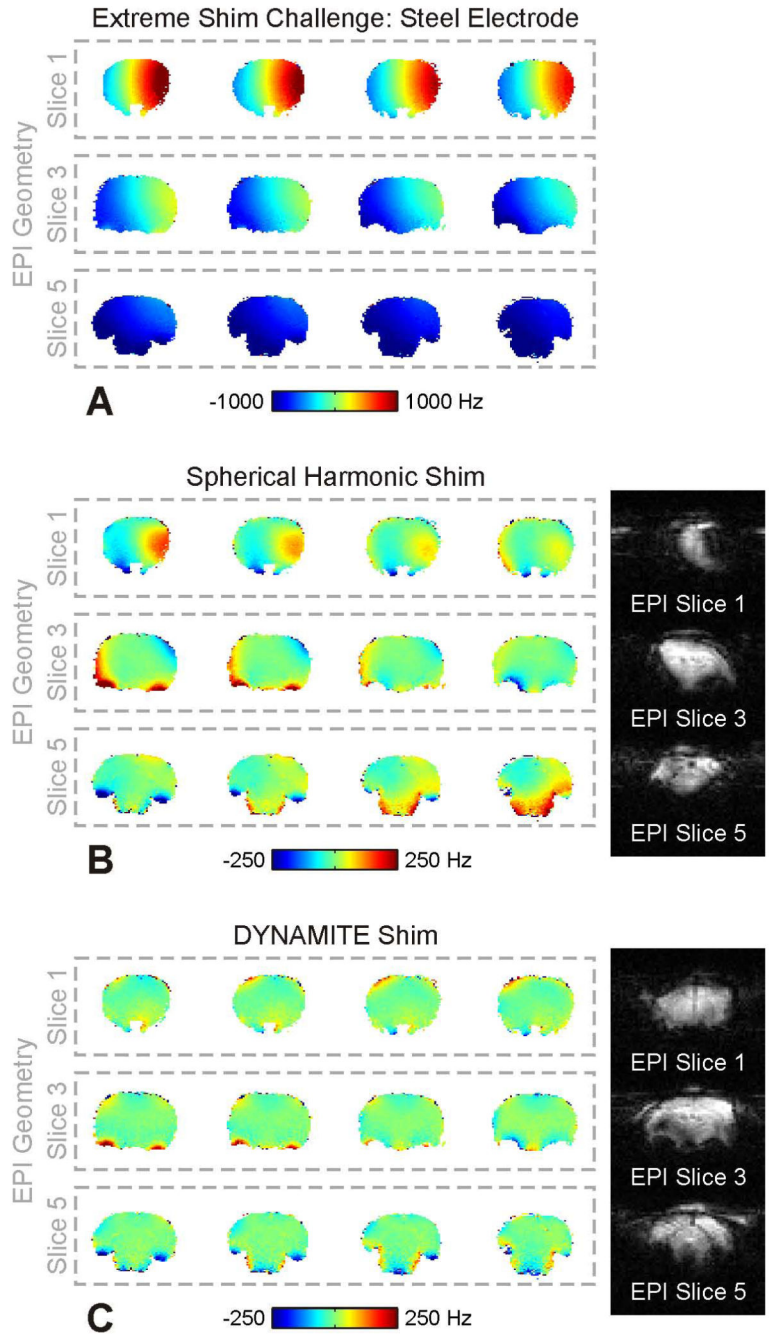

Fig. 6. EXTREME SHIM CHALLENGE – STEEL ELECTRODE

Extreme shim challenge. A: Magnetic field distribution with the use of a (magnetic) steel electrodes for whisker stimulation. For three 2-mm EPI slices the corresponding four 0.5-mm field maps are shown. A several thousand Hertz frequency spread is observed with both severe in-plane and through-plane components. B: While second order SH shimming removes the bulk of the distortion, significant field imperfections remain (left). The combination of in-slice imperfections and through-slice components, i.e. field variations across the four field maps contributing to the same EPI slice, lead to image distortion and

signal dropout with EPI (right). C: Single-step DYNAMITE shimming removed large part of the extreme field challenge (left) and, thereby, allowed reasonable EPI quality throughout the brain (right).

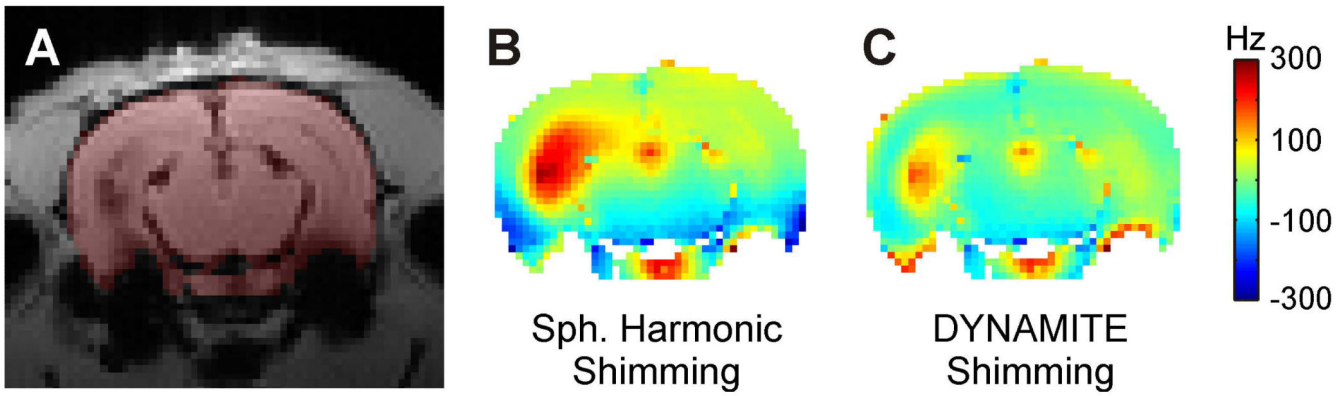

Fig. 7. OUTLOOK - METABOLIC IMAGING

Outlook of DYNAMITE shimming for specific research conditions: Molecular imaging with iron-oxide labeling. A: Rat brain after ventricular iron-oxide injection. The considered slice itself does not contain any iron load. B: While microscopic field distortions are desired with iron-oxide-based contrast agents to generate contrast, the concomitant macroscopic field alterations are not (residual field imperfection after theoretical SH shimming: SD 101 Hz). C: DYNAMITE field modeling and shimming is expected to mitigate these artifacts that can span over significant parts of the brain and to reduce signal dropout and image distortions (shim simulation for presented MC/RF implementation: SD 57 Hz).

Table 1

Homogeneity analysis of an example rat brain (Figs. 1/3) after magnetic field shimming. Major field imperfections remain after static third order SH shimming (Fig. 1) which is reflected by a large residual standard deviation (SD) and broad frequency ranges to cover 80%, 85%, 90% and 95% of the brain voxels (all values in Hertz). In comparison, DYNAMITE shimming removes most magnetic field imperfections in the rat brain (Fig. 3) and allows a substantial narrowing of the frequency distribution.

shim method	SD	80%	85%	90%	95%
static third order SH	58	116	136	171	231
DYNAMITE	22	35	45	60	91

Table 2

Magnetic field homogenization of a central 12 mm thick slab of the *in vivo* rat brain at 11.7 Tesla with different shimming techniques. Theoretical shimming including various spherical harmonic (SH) orders was applied statically and dynamically assuming unlimited amplitude range. DYNAMITE shimming was based on experimentally calibrated basis fields with the presented MC-RF setup including a ±1 A current limitation on all MC channels. The average standard deviation (mean ± SD) of the magnetic field distributions in 12 rat brains after shimming is reported.

uncorrected	**136 ± 20 Hz**
static SH 1st	69 ± 8 Hz
static SH 2nd	61 ± 11 Hz
static SH 3rd	52 ± 7 Hz
static SH 4th	44 ± 8 Hz
static SH 5th	38 ± 7 Hz
SH-DSU 1st	42 ± 4 Hz
SH-DSU 2nd	33 ± 4 Hz
SH-DSU 3rd	27 ± 3 Hz
SH-DSU 4th	22 ± 3 Hz
static MC shim	40 ± 5 Hz
DYNAMITE shim	17 ± 3 Hz